



Contents lists available at ScienceDirect

Bioorganic & Medicinal Chemistry Letters

journal homepage: www.elsevier.com/locate/bmcl

Discovery of potent, selective, and orally bioavailable inhibitors of interleukin-1 receptor-associate kinase-4



Zhulun Wang*, Daqing Sun*, Sheree Johnstone, Zhaodan Cao, Xiong Gao, Juan C. Jaen, Jingqian Liu, Sarah Lively, Shichang Miao, Athena Sudom, Craig Tomooka, Nigel P. C. Walker, Matthew Wright, Xuelei Yan, Qiuping Ye, Jay P. Powers

Amgen Inc., 1120 Veterans Boulevard, South San Francisco, CA 94080, USA

ARTICLE INFO

Article history:

Received 16 July 2015

Revised 17 October 2015

Accepted 20 October 2015

Available online 23 October 2015

Keywords:

Interleukin-1 receptor-associate kinase-4

N-Acyl-2-aminobenzimidazole

Inflammation

ABSTRACT

In this Letter, we report the continued optimization of the *N*-acyl-2-aminobenzimidazole series, focusing in particular on the *N*-alkyl substituent and 5-position of the benzimidazole based on the binding mode and the early SAR. These efforts led to the discovery of **16**, a highly potent, selective, and orally bioavailable inhibitor of IRAK-4.

© 2015 Elsevier Ltd. All rights reserved.

Interleukin-1 (IL-1) receptor-associated kinase-4 (IRAK-4) is a ubiquitously expressed serine/threonine kinase and is responsible for initiating signaling from Toll-like receptors (TLRs) and members of the IL-1/18 receptor family. IRAK-4 and its IRAK isoforms share a domain structure and activate similar signal transduction of NF- κ B and MAPK pathways.^{1–4} However, unlike the other IL-1 receptor-associated kinases (IRAK-1,¹ IRAK-2,² and IRAK-M³), IRAK-4 requires its kinase activity to activate NF- κ B.⁴ Endogenous IRAK-4 interacts with IRAK-1 and TRAF6 in an IL-1-dependent manner but is not redundant with IRAK-1, indicating that IRAK-4 may play a major role in the early signal transduction of Toll/IL-1 receptors. To this end, we found that mice with either IRAK-4 knockout or IRAK-4 targeted deletion had reductions in TLR and IL-1 induced pro-inflammatory cytokines and were resistant to induced joint inflammation in both antigen-induced arthritis (AIA) and serum transfer-induced (K/BxN) arthritis models.⁵ These results strongly suggest that IRAK-4 is indispensable for IL-1 signal transduction and its kinase activity is required for signal

Abbreviations: MeCN, acetonitrile; CL, clearance; Dess–Martin periodinane, 1,1,1-tris(acetyloxy)-1,1-dihydro-1,2-benziodoxol-3-(1H)-one; DIBALH, diisobutylaluminum hydride; DMF, *N,N*-dimethylformamide; EtOAc, ethyl acetate; HBTU, *N,N,N',N'*-tetramethyl-*O*-(1H-benzotriazol-1-yl)uronium hexafluorophosphate; HOBt, hydroxybenzotriazole; NMM, *N*-methylmorpholine; THF, tetrahydrofuran.

* Corresponding authors. Tel.: +1 650 244 2446; fax: +1 650 837 9427 (Z.W.); tel.: +1 650 619 1742; fax: +1 650 837 9427 (D.S.).

E-mail addresses: zwang@amgen.com (Z. Wang), daqingsun@yahoo.com (D. Sun).

<http://dx.doi.org/10.1016/j.bmcl.2015.10.060>

0960-894X/© 2015 Elsevier Ltd. All rights reserved.

transduction. Furthermore, human patients who lack full-length IRAK-4 expression suffer from a compromised immune response.⁶ Therefore, selective inhibition of IRAK-4 has emerged as a potential therapeutic strategy for the treatment of inflammatory pathologies such as atherosclerosis.^{7–12}

Previously, we reported the identification of a novel series of *N*-acyl-2-aminobenzimidazole IRAK-4 inhibitors exemplified by **1** (Fig. 1) from initial optimization efforts on an HTS lead.¹¹ Compound **1** inhibited both IRAK-4 and its isoform IRAK-1 in a chemiluminescent ELISA assay,¹³ with an IC₅₀ of 0.15 μ M and 0.9 μ M, respectively. The early structure–activity relationship (SAR) studies in this series¹³ identified the pharmacophore required for IRAK inhibition: (a) the secondary amide connection between the two aryl groups is favorable for potency as alkylation of the amide led to a substantial loss of activity, (b) both 3-nitro and 3-trifluoromethyl groups at the benzamide were beneficial for activity against IRAK-4, and (c) substitutions on the nitrogen and 5-positions of the benzimidazole significantly improved IRAK-4 inhibition.

Binding affinity of **1** to IRAK-4 can be explained by key interactions of three hydrogen bonds and van der Waals interactions, which were observed in the co-crystal structure of **1** with IRAK-4 (Fig. 2).¹⁴ As an ATP-site inhibitor, compound **1** makes a typical hinge hydrogen bond with the amide carbonyl accepting a hydrogen bond from the backbone amide of Met265. The nitro group forms a weak hydrogen bond with the side-chain NH₃⁺ of catalytic

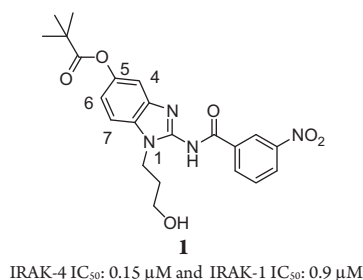


Figure 1. Structure and biochemical potency of **1**. Values of IC₅₀ are means of at least two determinations from a chemiluminescent ELISA assay.

Lys213 while the phenyl ring engages in a partial π - π aromatic stacking interaction with the gatekeeper, Tyr262. In addition, the pivalate ester is exposed to solvent and the carbonyl forms a non-conserved hydrogen bond with Arg273 of helix α D in the C-terminal lobe. Based on the aforementioned binding mode of **1** and associated SAR data, we decided to preserve the most important structural features for IRAK-4 binding and optimize substituents at the nitrogen and 5-position of the benzimidazole in order to improve potency, selectivity, and physicochemical properties.

Optimization of the benzimidazole N-alkyl substituent: Initial optimization of **1** began with modification of the benzimidazole N-alkyl substituent. Since the 3-nitro group of the benzamide interacts with Lys213 and the 5-substituent on the benzimidazole is favorable for IRAK-4 inhibition, 3-nitro-5-fluorobenzimidazole **2** (R = H, IC₅₀ = 4.5 μM, Table 1)¹¹ was used as a template for optimization. Adding a polar N-propanol group (**3**) improved potency by more than 100-fold, which was consistent with early SAR data (**3** vs **2**).¹¹ Increasing the size of the polar group from propanol to cyclohexanol led to a further improvement in potency. The *trans* N-cyclohexanol **4** (IC₅₀ = 6.5 nM) was almost six-fold more potent than **3** in the biochemical assay. Furthermore, expanding the N-cyclohexanol to an N-cyclohexylmethyl alcohol, produced compounds **5** and **6**. The *cis* isomer **5** was fourfold more potent than **4**, while the *trans* isomer **6** had potency similar to **4** in the biochemical assay. However, changing the ring size from six-membered to five-membered resulted in a slight loss of potency (**7** vs **5** and **8** vs **6**).

Optimization of the benzimidazole 5-position substituent: Although compounds such as **4** were of high potency, they suffered from poor solubility and permeability. Therefore, we introduced a

Table 1
Optimization of N-alkyl substituent of benzimidazole

Compound	R	IRAK-4 K _i ^a (nM)
2	H	4500
3	(CH ₂) ₃ OH	38.5
4		6.5
5		1.6
6		6.4
7		7.8
8		11

^a Values are means of at least two determinations.¹³

solubilizing group at the 5-position of the benzimidazole to improve the physicochemical properties. The cocrystal structure of **1** with IRAK-4 suggests that the pivalate ester projects out toward a solvent-exposed region and the carbonyl moiety acts as a hydrogen bond acceptor to Arg273. With these considerations in mind, a small group of analogs incorporating with hydroxyl, amine, and other solubilizing groups, were explored (Table 2). The 5-hydroxymethyl analog **9** was twofold less potent than **4** and showed no improvement in solubility or permeability. Gratifyingly, the piperidine analog **10** was more potent (IC₅₀ = 2.8 nM) than **4** and had improved solubility (50 μg/mL at pH 7.4) and permeability (6.6 × 10⁻⁶ cm/s). Interestingly, both morpholine **11** and lactam **12** were found to be more potent than **10** but with no significant improvement in permeability. The improved permeability of **10** may contribute to its low polar surface area.

Having identified the 5-piperidine as the key feature for potent IRAK-4 inhibition with good solubility and permeability, we turned our attention to selectivity over off-target enzymes. In general,

Table 2
Solubility and permeability data of analogs **9–12**

Compound	R	IRAK-4 K _i ^a (nM)	Solubility (pH = 7.4, μg/mL)	Permeability (10 ⁻⁶ cm/s)	PSA (Å ²)
9	HOCH ₂ C-	11	4.9	<1	137
10		2.8	>50	6.6	120
11		3.8	29	<1	129
12		0.5	0.8	<1	137

^a Values are means of at least two determinations.¹³

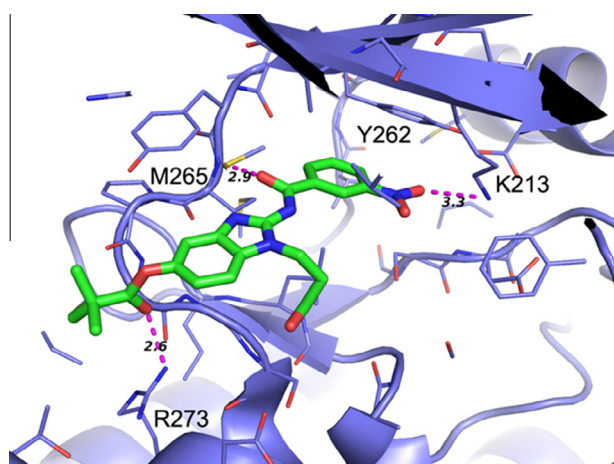
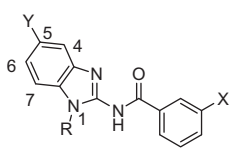


Figure 2. Co-crystal structure of **1** bound to IRAK-4 (2NRU.pdb).

Table 3
Potency and selectivity of selected analogs **10**, **13**–**19**



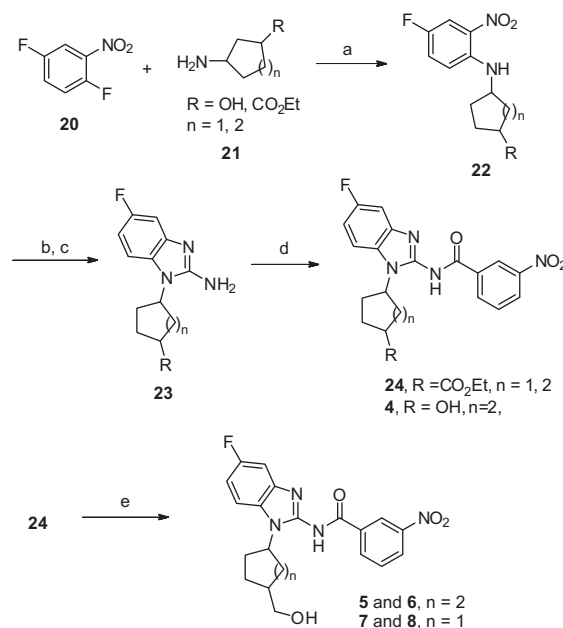
Compound	Y	R	X	IRAK-1 K_i^a (nM)	IRAK-4 K_i (nM)	TAK1 K_i (nM)	Ratio IRAK-1/IRAK-4	Ratio TAK1/IRAK-4	NF-kB EMSA IC_{50} (μ M)
10			NO ₂	18	2.8	15	6.4	5.3	ND
13			NO ₂	48	0.7	30	68	43	ND
14			CF ₃	72	0.42	130	171	310	<0.1
15			NO ₂	374	8.2	800	46	98	0.1
16			CF ₃	608	2.8	2500	217	892	0.3
17			CF ₃	12	1.3	700	9	538	<0.1
18			CF ₃	ND	0.34	2500	ND	7354	0.1
19	Y = H, 6-CH ₂ OH		CF ₃	ND	0.48	1300	ND	2708	<0.1

^a Values are means of at least two determinations.¹³

Table 4
Rat PK profiles of **10**, **13**, **16**, and **17**

Compound	Rat PK ^a			
	Cl (L/h/kg)	$T_{1/2}$ (h)	AUC (μ M)	F (po, %)
10	2.5	2.1	124	16
13	2.4	4.8	84	10
16	0.54	23.7	1023	46
17	2.2	1.3	175	19

^a Dosed iv at 0.5 mg/kg and po at 2.0 mg/kg.



Scheme 1. Reagents and conditions: (a) Et₂O, 30–36%; (b) H₂, Pd/C (5 wt %), EtOH, 91–96%; (c) CBr₄ (5.0 M in CH₃CN), MeOH/H₂O, 75–94%; (d) 3-nitrobenzoic acid, HBTU, HOBT, NMM, DMF, 57–60%; (e) DIBALH (1.0 M in toluene), THF, 57%.

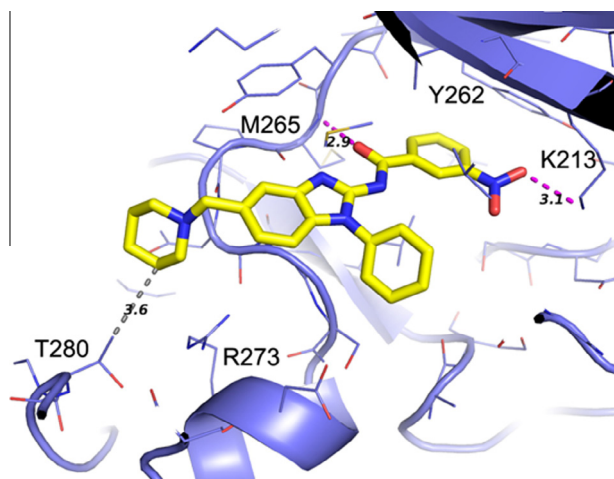
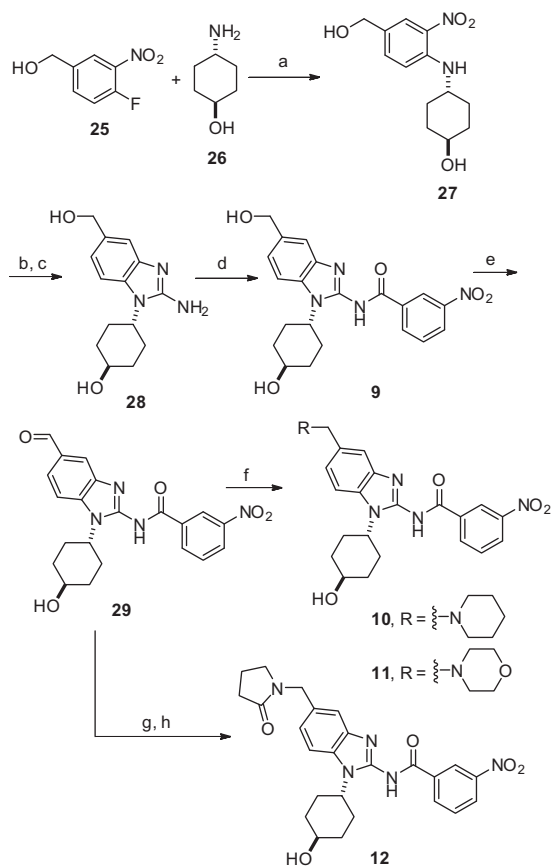


Figure 3. Co-crystal structure of **15** bound to IRAK-4.

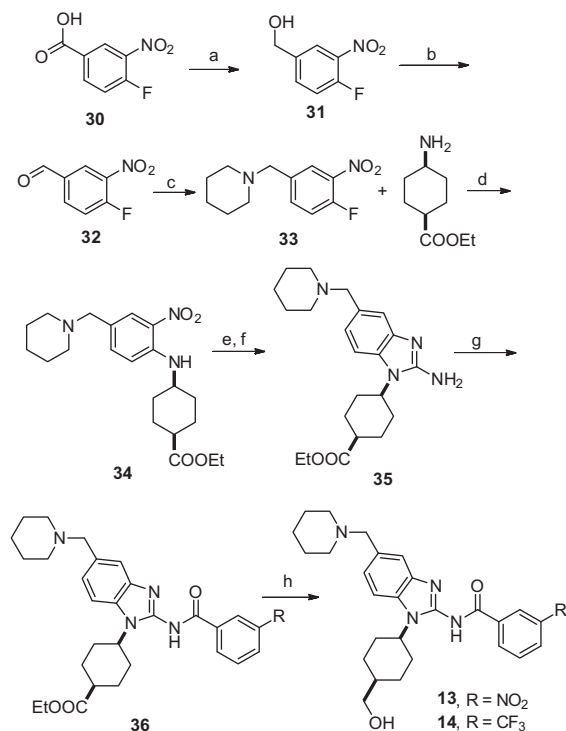
compound **10** showed >100 fold binding selectivity over a broad range of kinases including PKA, PKC, CDK2, CaMK, Akt1, EGFRK, pp60SRC, and LCK, and displayed poor selectivity against only two kinases: IRAK-1 and TAK1 (Table 3). Consistent with precedent, the *cis* *N*-cyclohexylmethyl alcohol **13** was fourfold more potent than **10** in the biochemical assay and showed improvement



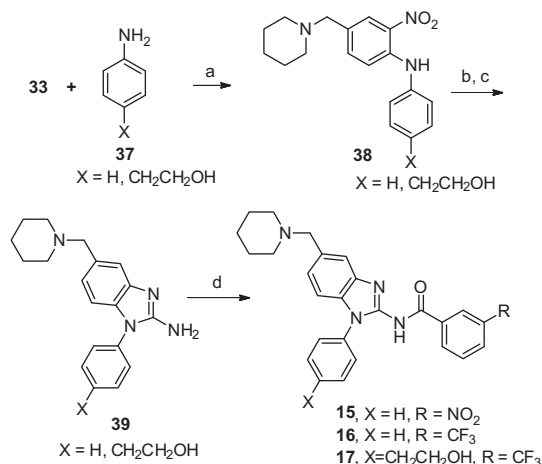
Scheme 2. Reagents and conditions: (a) *N,N*-diisopropylethylamine, 90 °C, 29%; (b) cyclohexene, Pd/C (5 wt %), EtOH, reflux; (c) CBrN (5.0 M in CH₃CN), MeOH/H₂O; (d) 3-nitrobenzoic acid, HBTU, HOBT, NMM, DMF, 15% from **27**; (e) Dess–Martin periodinane, THF, 58%; (f) piperidine or morpholine, NaBH(OAc)₃, acetic acid, 1,2-dichloroethane, 58–62%; (g) ethyl 4-aminobutyrate, NaBH(OAc)₃, NaOAc, AcOH/MeOH, 57%; (h) reflux, toluene/acetic acid, 85%.

in selectivity. Changing the substituent at the 3-position of the benzamide from a nitro to trifluoromethyl (**14**) led to further improvement of potency and selectivity against kinases IRAK-1 (68-fold for **13** vs 171-fold for **14**) and TAK1 (43-fold for **13** vs 310-fold for **14**). Replacement of the *N*-cyclohexanol with an *N*-phenyl group produced analogs **15** and **16**. The 3-trifluoromethyl **16** had maintained potency along with improved selectivity against IRAK-1 (6.4-fold for **10** vs 217-fold for **16**) and TAK1 (5.3-fold for **10** vs 892-fold for **16**) compared to **10**. Expanding the *N*-phenyl group to *N*-phenylethanol **17** led to slight improvement in potency but substantial decreased selectivity against IRAK-1 when compared to **16**. Interestingly, replacing the piperidine with an amide (**18**) significantly improved the selectivity against TAK1. A substituent at the 6-position of benzimidazole, as exemplified by **19**, also showed great improvement in selectivity. Furthermore, we evaluated the ability of compounds **14**–**19** to inhibit IL-1 induced activation of NF-κB in primary human monocytes. In this cellular assay, all compounds were found to inhibit the activation of NF-κB with low submicromolar activity (Table 3).

Encouraged by potent in vitro inhibition of IRAK-4 and improved selectivity, we profiled compounds **10**, **13**, **16**, and **17** in rat pharmacokinetic studies. As shown in Table 4, compound **16** had the lowest in vivo clearance of 0.54 L/h/kg with a long half-life ($T_{1/2}$ = 23.7 h), and good oral bioavailability (%F = 46), while the compounds **10**, **13**, and **17** had high clearance (2.2–2.5 L/h/kg) and lower oral exposure (10–19%). In mice pharmacokinetic studies, compound **16** displayed moderate clearance (CL = 1.2 L/h/kg) and high oral exposure (%F = 89).



Scheme 3. Reagents and conditions: (a) 1.0 M BH₃·THF, THF, 90%; (b) NaOCl, tempo, KBr, CH₂Cl₂/H₂O; 91%; (c) piperidine, NaBH(OAc)₃, acetic acid, 1,2-dichloroethane, 57%; (d) *N,N*-diisopropylethylamine, 110 °C, 15%; (e) SnCl₂·2H₂O, EtOAc/EtOH, 100 °C, 91%; (f) CBrN (5.0 M in CH₃CN), MeOH/H₂O, 90%; (g) 3-nitrobenzoic acid or 3-trifluoromethylbenzoic acid, HBTU, HOBT, NMM, DMF, 46–48%; (h) DIBALH (1.0 M in toluene), THF, 63%.



Scheme 4. Reagents and conditions: (a) *N,N*-diisopropylethylamine, 150 °C, 77%; (b) SnCl₂·2H₂O, reflux, EtOAc/EtOH; (c) CBrN (5.0 M in CH₃CN), MeOH/H₂O; (d) nitrobenzoic acid or 3-trifluoromethyl benzoic acid, HBTU, HOBT, NMM, DMF, 18% from **38**.

We also determined the co-crystal structure of compound **15** with IRAK-4 to a resolution of 2.2 Å (Fig. 3).¹⁵ Compound **15** maintained the identical interactions to the hinge Met265, the catalytic Lys213, and the gatekeeper Tyr262 as compared with compound **1**. However, the 5-piperidine moiety does not form any hydrogen bond interactions with Arg273, instead it forms numerous van der Waals contacts with the mouth cleft formed by Asn267 in the hinge, helix αD and the loop DE especially through residue Thr280. Note that Arg273 is conserved between IRAK-4 and

IRAK-1, while Thr280 of IRAK-4 corresponds to Cys308 in IRAK-1. In addition, the *N*-phenyl moiety also forms good van der Waals contacts with strand β 1, including Met192 which is also a non-conserved residue between IRAK-4 and IRAK-1 (corresponding residue Ile218). The structural data provided a molecular basis for the improved selectivity of compound **15** towards IRAK-4 over IRAK-1 and substantiated our SAR direction.

Compounds **4–19** were synthesized via the routes outlined in Schemes 1–4. The synthesis of **4–8**, is detailed in Scheme 1. Treatment of 1,4-difluoro-2-nitrobenzene (**20**) with excess amine **21** at room temperature produced aniline **22**. Hydrogenation of **22** followed by treatment with cyanogen bromide gave 2-aminobenzimidazole **23**. Coupling reaction of **23** with 3-nitrobenzoic acid afforded alcohol **4** or esters **24**, respectively. Finally, ester **24** was reduced with DIBALH to yield alcohols **5–8**. Compounds **18** and **19** were prepared using a similar procedure described in Scheme 2, substituting (4-fluoro-3-nitrophenyl) pivalamide or 3-fluoro-4-nitrophenylmethanol with **20**.

In a similar fashion, 5-hydroxymethyl analog **9** was prepared from 4-fluoro-3-nitrophenylmethanol **25** and 4-aminocyclohexanol **26** as shown in Scheme 2. Oxidation of **9** with Dess–Martin periodinane resulted in aldehyde **29**, which was subjected to reductive amination with the appropriate amines to afford compounds **10**, **11**, and **12**.

As shown in Scheme 3, compounds **13** and **14** were synthesized from intermediate **33**, which was prepared from benzoic acid **30** using a series of common transformations. Direct nucleophilic displacement between **33** and (1*S*,4*S*)-ethyl 4-aminocyclohexanecarboxylate, was followed by reduction benzimidazole formation and amide coupling reaction, as before, to produce ester **36**. Finally, ester **36** was reduced with DIBALH to form compounds **13** and **14**. Similarly, compounds **15–17** were prepared from the intermediate **33** and the appropriate anilines **37** (Scheme 4).

In summary, the extensive optimization of the *N*-alkyl substituent and 5-position of the benzimidazole in the *N*-acyl-2-aminobenzimidazole series led to the discovery of **16**, a potent, selective, and orally bioavailable inhibitor of IRAK-4. The enhanced

potency and selectivity of **16** can be rationalized by the improved van der Waals interactions with IRAK-4, especially to those non-conserved residues between IRAK-4 and IRAK-1, which were observed in the co-crystal structure of **15** bound to IRAK-4. With a combination of high potency, excellent selectivity and pharmacokinetic properties, compound **16** may be a useful tool to investigate inhibition of IRAK-4 in efficacy models.

References and notes

1. Cao, Z.; Henzel, W. J.; Gao, X. *Science* **1996**, *271*, 1128.
2. Muzio, M.; Ni, J.; Feng, P.; Dixit, V. M. *Science* **1997**, *278*, 1612.
3. Wesche, H.; Gao, X.; Li, X.; Kirschning, C. J.; Stark, G. R.; Cao, Z. *J. Biol. Chem.* **1999**, *274*, 19403.
4. Li, S.; Strelow, A.; Fontana, E. J.; Wesche, H. *Proc. Natl. Acad. Sci. U.S.A.* **2002**, *99*, 5567.
5. Koziczak-Holbro, M.; Littlewood-Evans, A.; Pollinger, B.; Kovarik, J.; Dawson, J.; Zenke, G.; Burkhart, C.; Muller, M.; Gram, H. *Arthritis Rheum.* **2009**, *60*, 1661.
6. Hernandez, M.; Bastian, J. F. *Curr. Allergy Asthma Rep.* **2006**, *6*, 468.
7. Wang, Z.; Wesche, H.; Stevens, T.; Walker, N.; Yeh, W.-C. *Curr. Top. Med. Chem.* **2009**, *9*, 724.
8. Buckley, G. M.; Fosbeary, R.; Fraser, J. L.; Gowers, L.; Higuieruelo, A. P.; James, L. A.; Jenkins, K.; Mack, S. R.; Morgan, T.; Parry, D. M.; Pitt, W. R.; Rausch, O.; Richard, M. D.; Sabin, V. *Bioorg. Med. Chem. Lett.* **2008**, *18*, 3656.
9. Buckley, G. M.; Ceska, T. A.; Fraser, J. L.; Gowers, L.; Groom, C. R.; Higuieruelo, A. P.; Jenkins, K.; Mack, S. R.; Morgan, T.; Parry, D. M.; Pitt, W. R.; Rausch, O.; Richard, M. D.; Sabin, V. *Bioorg. Med. Chem. Lett.* **2008**, *18*, 3291.
10. Buckley, G. M.; Gowers, L.; Higuieruelo, A. P.; Jenkins, K.; Mack, S. R.; Morgan, T.; Parry, D. M.; Pitt, W. R.; Rausch, O.; Richard, M. D.; Sabin, V.; Fraser, J. L. *Bioorg. Med. Chem. Lett.* **2008**, *18*, 3211.
11. Powers, J. P.; Li, S.; Jaen, J. C.; Liu, J.; Walker, N. P. C.; Wang, Z.; Wesche, H. *Bioorg. Med. Chem. Lett.* **2006**, *16*, 2842.
12. Tumej, L. N.; Boschelli, H. D.; Bhagirath, N.; Jaechul Shim, J.; Murphy, A. E.; Goodwin, D.; Bennett, M. E.; Wang, M.; Lin, L.; Press, B.; Shen, M.; Frisbie, K. R.; Morgan, P.; Mohan, S.; Shin, J.; Rao, R. V. *Bioorg. Med. Chem. Lett.* **2014**, *24*, 2066.
13. IRAK-4 enzyme activity was determined by its ability to phosphorylate a biotinylated synthetic peptide substrate (RRRVTSPPARRS, sequence derived from GFAP) in a chemiluminescent ELISA. Assays were performed in streptavidin-coated 96-well plate format utilizing recombinant full length IRAK-4 and 10 μ M ATP. K_i values for inhibition of IRAK-4 were calculated from a minimum of two separate determinations each performed in duplicate.
14. Wang, Z.; Liu, J.; Athena Sudom, A.; Ayres, M.; Shyun Li, S.; Wesche, H.; Powers, J. J.; Walker, P. C. N. *Structure* **2006**, *14*, 1835.
15. Co-crystal structure of **15** with IRAK-4 has been deposited in RCSB Protein Data Bank under accession code 4RMZ.